Journal of Physics: Conference Series **770** (2016) 012010 doi:10.1088/1742-6596/770/1/012010

The KLOE-2 Experiment at DAΦNE

A De Santis[1]

INFN - Laboratori Nazionali di Frascati, v. Enrico Fermi, 50, 00044

E-mail: antonio.desantis@lnf.infn.it

Abstract. The KLOE-2 experiment is currently collecting data at DAΦNE the INFN e^+e^- collider located in the Frascati National Laboratories.

The experiment has a wide physics program ranging from: discrete symmetries test, study of light unflavored mesons, searches for light mass for dark matter candidates.

In this contribution the upgrade of the detector will be briefly discussed before starting a more detailed presentation on some results concerning: CPT and Lorentz Invariance tests with neutral kaons, dark forces massive boson mediator searches, hadron structure and low energy mesons interaction.

1. KLOE-2 Experiment

The KLOE-2 experiment [1] is currently taking data at DAΦNE collider [2][3], the e^+e^- accelerator of the Frascati National Laboratory running at the ϕ resonance peak. DAΦNE began operations for KLOE-2 experiment in November 2014 with a new Crab-Waist collision scheme and customized permanent magnet optics in the interaction region [4] to increase the specific luminosity. Several consolidation intervention [5] allowed to deliver 3.0 fb^{-1} integrated luminosity: 2.4 fb^{-1}acquired that corresponds to 7.4 billion of ϕ decays. A record peak-luminosity of 2.21×10^{32} cm^{-2}s^{-1} has been achieved. The best daily integrated luminosity has been 13.4 pb^{-1} and the best weekly integrated luminosity has been 76.3 pb^{-1}. Full time evolution of data delivery is shown in figure 1.

The KLOE-2 experiment is an upgraded version of the previous KLOE apparatus with the inclusion of new sub-detectors allowing for larger physics program with increased reconstruction performance. The original KLOE detector consists of a large cylindrical drift chamber (DC) [6] surrounded by a lead-scintillating fiber electromagnetic calorimeter (EMC) [7]. A superconducting coil around the EMC provides a 0.52 T axial field.

Two pairs of electron-positron taggers have been installed for $\gamma\gamma$ physics: a small LYSO crystal calorimeter matrix, the Low Energy Tagger [8] inside KLOE-2 apparatus and a plastic scintillator hodoscope, the High Energy Tagger (HET) [9], along the beam lines outside KLOE-2 detector.

To increase the acceptance two new calorimeters have been developed. A pair of LYSO crystal calorimeters (CCALT) [10] have been installed near the interaction region to cover the low-θ range. This calorimeter will be also useful to provide fast signals for luminosity measurement and beam instability feedback to help DAFNE tune-up [11].

[1] on behalf of KLOE-2 Collaboration

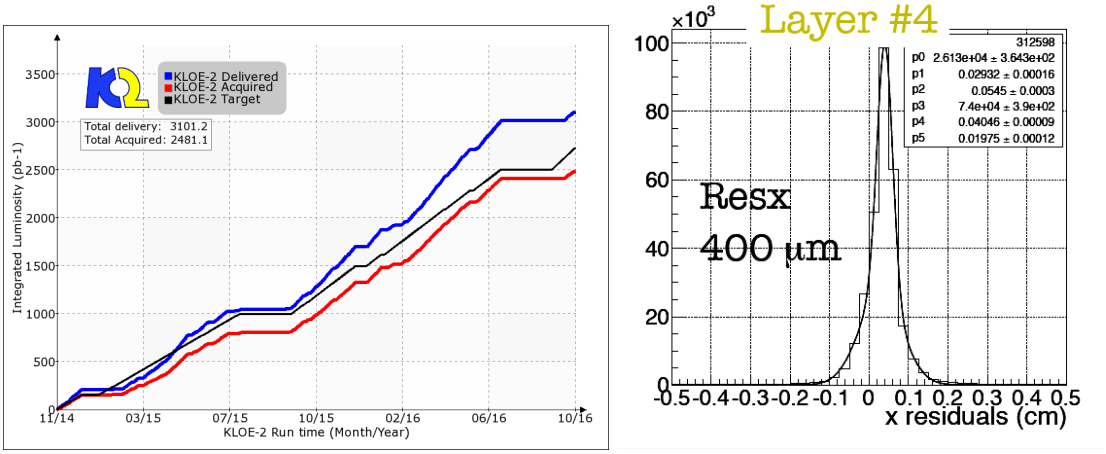

Figure 1. Left: time evolution of the DAΦNE data delivery since November 2014. The blue line represent the integrated luminosity delivered, while the red curve is the corresponding amount of integrated luminosity acquired. The black line represent the target luminosity fixed to achieve KLOE-2 goal of 5 fb^{-1} by the end of KLOE-2 physics run. The black line is horizontal during DAΦNE planned shut-downs (maintenance/laboratory closure). Riht: preliminary results on the residuals between observed and projected impact point with Bhabha scattering events on the outermost plane of the IT. The width of this distribution is the convolution of the IT and DCH resolutions.

A pair of tile calorimeters (QCALT) [12], covers the quadrupoles inside KLOE-2 detector and along the beam pipe. These calorimeters are made of tungsten slabs and singly read-out scintillator tiles to improve the angular coverage for particles coming from the active volume of the DC (e.g. K_L decay).

The most important and challenging upgrade is a multilayer cylindrical GEM [13] tracker for the reconstruction of decay in the vicinity of the primary interaction point (IP). Inner Tracker (IT) is made of four planes covering the tranverse radius interval between 10 and 25 cm from KLOE-2 center. It is expected to double decay vertex resolution at the IP. The current status of alignment of this detector is shown in figure 1.

2. Kaon interferometry

Entangled neutral kaon pair can be observed at KLOE-2 because ϕ decay via strong interaction preserves the ϕ quantum numbers: $J^{PC} = 1^{--}$. For an exhaustive review on this topic refer to [14]. The initial state $|\phi\rangle \propto |K_S, \vec{p}\rangle|K_L, -\vec{p}\rangle - |K_S, -\vec{p}\rangle|K_L, \vec{p}\rangle$ evolves preserving the correlation. Observing the two kaons decaying in the same final state ($\pi^+\pi^-$) as a function of the difference of proper decay times (Δt) the following distribution is expected:

$$I_{f_1 f_2}(\Delta t) \propto e^{-\Gamma_\Sigma |\Delta t|}\left[|\eta_1|^2 e^{\frac{\Delta\Gamma}{2}\Delta t} + |\eta_{f_2}|^2 e^{-\frac{\Delta\Gamma}{2}\Delta t} - 2|\eta_1||\eta_2|\cos(\Delta m \Delta t + \Delta\phi_{12})\right] \quad (1)$$

where $\Gamma_\Sigma = \Gamma_S + \Gamma_L$, $\Delta\Gamma = \Gamma_S - \Gamma_L$, $\Delta m = m_{K_L} - m_{K_S}$ and $\eta_j = \langle\pi^+\pi^-|K_L(\vec{P}_j)\rangle / \langle\pi^+\pi^-|K_S\rangle = \varepsilon_K - \delta_K$, where ε_K and δ_K are the CP and CPT violation parameters in the kaon system, respectively. According to the Standard Model Extension (SME) framework [15] and Greenberg theorem [16], the δ_K parameter is expressed as:

$$\delta_K \equiv \delta_K(P_\mu) \approx i \sin\phi_{SW} e^{i\phi_{SW}} \frac{E_K}{m_K}(\Delta a_0 - \frac{\vec{P}_K}{E_K} \cdot \Delta\vec{a})/\Delta m, \quad (2)$$

where P_μ is the kaon 4-momentum, ϕ_{SW} is the super-weak phase and Δa_μ are the SME parameters for the kaon system that explicitly violates Lorentz invariance.

At KLOE-2 the two kaons are produced almost back-to-back in the ϕ decay and therefore evolve with two different δ_K ($\delta_{\rm K}(\tilde{\rm P}_1) \neq \delta_{\rm K}(\tilde{\rm P}_2)$), this induces small asymmetries in the equation 1 that are expected to be modulated by the Earth rotation if the kaon momentum is observed in a reference frame defined by fixed stars. The data distributions have been fitted including SME effects to extract Δa_μ as show in figure 2

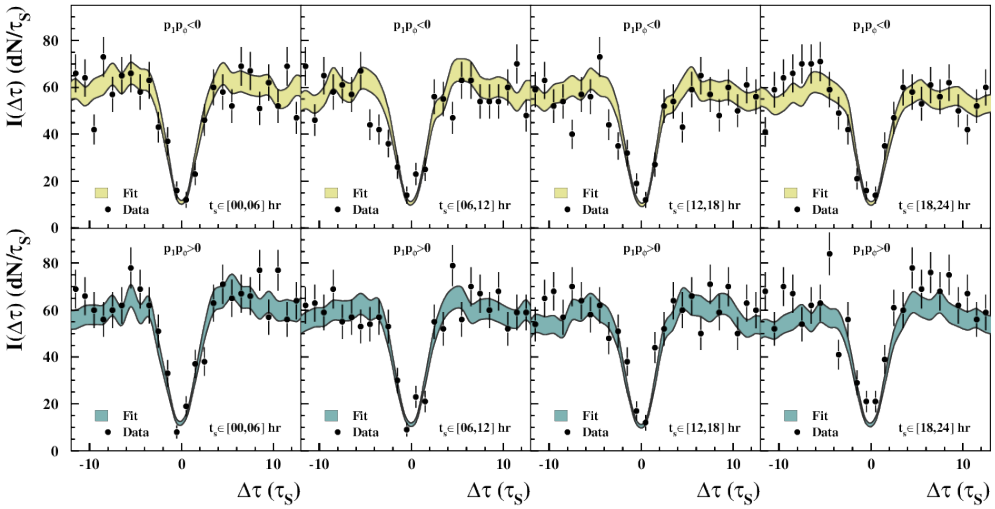

Figure 2. Fit results for Δa_μ parameters. left and right columns are relative to different angular selection in the laboratory frame while rows refers to different sidereal time interval. Black points are data while colored bands are the fit output. The fit $\chi^2/N_{\rm DoF}$ is 211.7/187 corresponding to a probability of 10%.

The results for the Δa_μ parameters, in 10^{-18} GeV units, are [17]: $\Delta a_0 = (-6.0 \pm 7.7_{stat} \pm 3.1_{syst})$, $\Delta a_{\rm X} = (0.9 \pm 1.5_{stat} \pm 0.6_{syst})$, $\Delta a_{\rm Y} = (-2.0 \pm 1.5_{stat} \pm 0.5_{syst})$, $\Delta a_{\rm Z} = (3.1 \pm 1.7_{stat} \pm 0.5_{syst})$. That are the most precise result in the quark sector of the SME. The total error is fully dominated by the statistical uncertainty.

3. Dark forces searches

Several astrophysical observations have obtained results not fitting the Standard Model (SM) framework [18]. To explain these anomalies a new gauge U(1) interaction mediated by a massive vector gauge boson, the U boson (dark photon), with mass below two proton masses and kinetically mixed with the SM U(1) hypercharge gauge field has been proposed. The small coupling between dark matter and the SM is described by a single kinetic mixing parameter: $\epsilon(= \alpha_D/\alpha_{EW})$.

Depending on the interaction type, the U bosons should appear as a sharp resonance at m_U in the invariant-mass distributions of final-state particles in reactions of the type $e^+e^- \to U\gamma$ with $U \to X^+X^-(X = e/\mu/\pi)$ or in meson Dalitz decays.

At KLOE two different searches [19] were performed using the decay chain $\phi \to \eta U$ with $U \to e^+e^-$ and $\eta \to \pi^+\pi^-\pi^0$ and $\eta \to \pi^0\pi^0\pi^0$ using 1.7 fb^{-1}of data. Irreducible background from Dalitz decay $\phi \to \eta e^+e^-$ was studied separately, as discussed in the next section. A resonant peak was not observed and the CLS technique [20] was used to set an upper limit on the strength of kinetic mixing parameter as a function of the U boson mass. The 90% confidence level limit is shown in figure 3.

KLOE data have been used to search for all the two body decays: $U \to X^+X^-(X = e/\mu/\pi)$. For the $U \to \mu^+\mu^-$ process [21] and $U \to \pi^+\pi^-$ [24] the two charged tracks are required to be emitted at large-angle (detected in the EMC barrel) while the initial-state radiation (ISR) photon is not detected. For the e^+e^- final state [23] all the particles are observed at large-angle.

In all the three analysis the final invariant mass spectrum was obtained after subtracting residual background obtained form Monte-Carlo (MC) simulation normalized with dedicated data control samples. No resonant peak was observed so the CLS technique was used to estimate the maximum number of U boson signal events that can be excluded at 90% confidence level, N_{CLS} as a function of the U invariant mass. This upper limit translate in the corresponding value for the ϵ parameter as shown in figure 3.

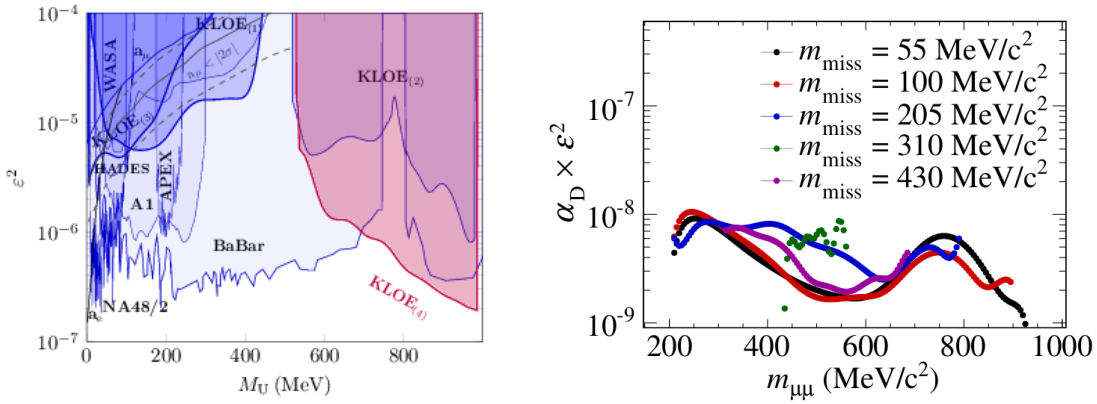

Figure 3. Left: summary of 90% CL exclusion limits on the dark sector coupling as a function of the U boson invariant mass. In the plot label KLOE(1) is for the combination of the results relative to $\phi \to \eta\gamma$ [19], KLOE(2) and KLOE(3) is relative to $\mu^+\mu^-\gamma$ [21] and $e^+e^-\gamma$ [23] final state, respectively. KLOE(4) is for the $\pi^+\pi^-\gamma$ final state [24]. KLOE-2 results are also compared with the exclusion plots obtained by other experiments [22]. Right: Limits from dark Higgs-strahlung process. The limit is presented as a function of the dilepton invariant mass (m_U) for different values of the event missing mass (dark Higgs mass). Lines represents the exclusion plots at the 90% CL.

A different scenario has been considered: the U(1) gauge symmetry is spontaneously broken by a Higgs-like mechanism, thus implying the existence of at least one other scalar particle, h' [25]. The hypothetical dark Higgs-strahlung process $e^+e^- \to Uh'$ with $U \to \mu\mu$ has been investigated using KLOE data [26].

Assuming $m_{h'} < m_U$ the dark Higgs boson would have a large lifetime and escape KLOE detector without interacting. 1.65 fb^{-1} of data collected at the ϕ-peak energy, and 0.2 fb^{-1} of data at 1 GeV energy have been used. A sharp peak in the two-dimensional distribution missing mass versus $m_{\mu\mu}$ is expected for the signal. No evidence of the dark Higgs-strahlung process was found. Using uniform prior distributions, 90% confidence level Bayesian upper limits on the number of events, $N_{90\%}$, were derived separately for the two samples used and then combined. The combined 90% confidence level limits are shown figure 3.

4. Hadron physics

The low-energy structure of hadrons is strongly connected with precise knowledge of meson transition form factors (TFF) that are also connected in the determination of the "light-by-light" contribution to the anomalous magnetic moment of the muon, one the largest source of uncertainty in the $(g-2)_\mu$ calculation [27].

KLOE-2 collaboration has measured the $\phi \to \eta$ and $\phi \to \pi^0$ TFFs studying the decays $\phi \to \eta(3\pi^0)\mathrm{e}^+\mathrm{e}^-$ [28] and $\phi \to \pi^0\mathrm{e}^+\mathrm{e}^-$ [29]. In figure 4 the TFFs are shown as a function of $\sqrt{q^2} = m_{ee}$, the invariant mass of e^+e^- system. The observed mass spectrum has been described according to [30] where the TFF is included with a single pole parametrization, $|F_{\phi\eta}(q^2)|^2 = (1 - q^2/\Lambda^2)^{-1}$. The Λ parameter is extracted from the m_{ee} invariant mass spectrum and the corresponding slope parameter ($\mathrm{b}_{\phi\eta} = \frac{\mathrm{dF(q^2)}}{\mathrm{dq^2}}|_{\mathrm{q^2=0}} = \Lambda^{-2}$) is evaluated. The value $\mathrm{b}_{\phi\eta} = 1.17 \pm 0.10^{+0.07}_{-0.11}\,\mathrm{GeV}^{-2}$ has been obtained while $1\mathrm{GeV}^{-2}$ is expected by pure VMD description. In the analysis has been measured also the branching fraction $\mathrm{B}(\phi \to \eta\mathrm{e}^+\mathrm{e}^-) = 1.075 \pm 0.007 \pm 0.038) \times 10^{-4}$.

For the decay $\phi \to \pi^0 e^+e^-$, using the same parametrization [30], the invariant mass spectrum has been fitted and a slope of $\mathrm{b}_{\phi\pi^0} = 2.02 \pm 0.11\,\mathrm{GeV}^{-2}$ has been obtained. Naive VMD extimate would give $\mathrm{b}_{\phi\pi^0} \sim 1\,\mathrm{GeV}^{-2}$, while prediction based on disperve calculation [31] are $\mathrm{b}_{\phi\pi^0} \sim 2.52 \ldots 2.68\,\mathrm{GeV}^{-2}$.

The branching fraction $B(\phi \to \pi^0 e^+e^-) = (1.035 \pm 0.005^{+0.05}_{-0.10}) \times 10^{-5}$ has been measured.

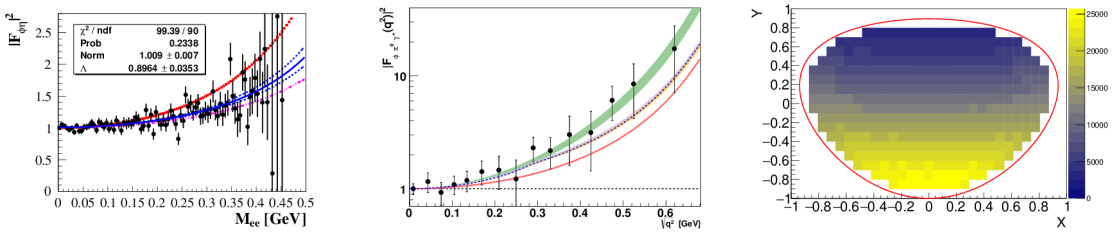

Figure 4. TFF $|F_{\phi P}(q^2)|^2$ as a function of $\sqrt{q^2}$ (invariant mass of e^+e^-) for $\phi \to \eta\mathrm{e}^+\mathrm{e}^-$ (left) and $\phi \to \pi^0\mathrm{e}^+\mathrm{e}^-$ (center). Black dots are data. In the top panel the blue curve is the single pole approximation of the TFF with the slope measured on the m_{ee} mass spectrum. Red and purple are different theoretical model: Terschluensen/Leupold [32] and VMD, respectively. In the bottom panel the green band is the Ivashyn model [31], the red curve is the VMD expectation, while the dashed line is KLOE-2 fit result. Right: Dalitz density distribution as a function of $X = \sqrt{3}\frac{T_{\pi^+} - T_{\pi^-}}{Q_\eta}$ and $Y = \frac{3T_{\pi^0}}{Q_\eta} - 1$ and $Q_\eta = m_\eta - 2m_{\pi^+} - m_{\pi^0}$.

Recently a new result on the $\eta \to \pi^+\pi^-\pi^0$ Dalitz plot density with the highest statistics in the world ($\sim 4.5 \cdot 10^6$ events) [33] has been released. This analysis allows to extract the light quark mass difference and to perform a test of the charge conjugation violation. The η decay is selected among the $\phi \to \eta\gamma$ radiative decay events having two tracks and two extra gamma's. The density of the Dalitz plot as a function of the kinetic energies of the pions is then fitted with a polynomial:

$$|A(X,Y)|^2 = \mathcal{N}(1 + aY + bY^2 + cX + dX^2 + eXY + fY^3 + gX^2Y + \ldots) \qquad (3)$$

where X and Y are the normalized Dalitz plot variables. The equation 3 should be symmetric under X parity (charge conjugation) thus resulting in $c = e = 0$, confirmed by data. Fitting the distribution show in figure 4 KLOE-2 obtained the following results for the non-vanishing coefficients:

$$a = -1.095 \pm 3 \pm 2;\ b = 0.145 \pm 3 \pm 5;\ \mathrm{d} = 0.081 \pm 3^{+5}_{-6};$$

$$\mathrm{f} = 0.141 \pm 7^{+7}_{-8};\ \mathrm{g} = -0.044 \pm 9^{+12}_{-13}$$

The g parameter has been observed different from zero for the first time because of the high statistics collected and high purity of the signal selected.

5. Conclusions

The data delivery evolution, shown in figure 1, demonstrates DAΦNE capabilities to fulfill the physics run goal within the allocated time: 5 fb^{-1} within 2017. The KLOE-2 detector is fully functional and all subdetectors are constantly monitored in order to keep the detector fully calibrate and perfectly operational during the whole data taking period as well as the DAΦNE performance.

Waiting for the full understanding of the new collected data, KLOE-2 collaboration progress in the study of the original KLOE dataset producing interesting physics results with the aim of use the new analysis on the old data as benchmark for the new data especially on the $\gamma\gamma$ physics and kaon interferometry.

6. References

[1] G. Amelino-Camelia *et al.*, Eur. Phys. J. C **68** (2010) 619
[2] G. Vignola et al., Frascati Phys. Ser. 4:19-30, 1996.
[3] P. Raimondi et al., arXiV:physics/0702033; C. Milardi et al., Int.J.Mod.Phys.A24:360-368, 2009; M.
[4] C. Milardi et al 2012 JINST 7 T03002.
[5] C. Milardi et al, THPRI002, IPAC14 (2014); A. De Santis et al, THPRI015, IPAC14 (2014); C. Milardi et al, WEOCA03, IPAC14 (2014).
[6] M. Adinolfi *et al.*, [KLOE],NIM A 488 (2002) 51.
[7] M. Adinolfi *et al.*, [KLOE],NIM A 482 (2002) 363.
[8] D. Babusci *et al.*, NIM A **617**, 81 (2010).
[9] F. Archilli, *et al.*, NIM A **617** (2010) 266.
[10] F. Happacher *et al.*, Nucl. Phys. Proc. Suppl. **197**, 215.
[11] A. De Santis DAΦNE Tech. Note BM-18 (2016).
[12] M. Cordelli *et al.*, NIM A **617**, 105 (2010).
[13] A. Balla, *et al.*, NIM A **628** (2011) 194
[14] A. Di Domenico, Frascati Physics Series, Vol. 43 (2007)
[15] V. A. Kostelecky, Phys. Rev. D **64** (2001) 076001
[16] O. W. Greenberg, Phys. Rev. Lett. **89** (2002) 231602.
[17] D. Babusci *et al.* [KLOE-2 Collaboration], Phys. Lett. B **730**, 89 (2014)
[18] O. Adriani, et al., Nature 458 (2009) 607. P. Jean, et al., Astron. Astrophys. 407 (2003) L55. J. Chang, et al., Nature 456 (2008) 362. HESS Coll., Phys. Rev. Lett. 101 (2008) 261104. HESS Coll., Astron. Astrophys. 508 (2009) 561. A. A. Abdo, et al., Phys. Rev. Lett. 102 (2009) 181101. R. Bernabei, et al., Int. J. Mod. Phys. D 13 (2004) 2127. R. Bernabei, et al., Eur. Phys. J. C 56 (2008) 333. CoGeNT Coll., Phys. Rev. Lett. 106 (2011) 131301. CoGeNT Coll., Phys. Rev. Lett. 107 (2011) 141301. AMS Coll., Phys. Rev. Lett. 110 (2013) 141102.
[19] KLOE-2 Coll., Phys. Lett. B 706 (2012) 251255. KLOE-2 Coll., Phys. Lett. B 720 (2013) 111115.
[20] G. C. Feldman, R. D. Cousins, Phys. Rev. D 57 (1998) 3873.
[21] KLOE-2 Coll., Phys. Lett. B 736 (2014) 459464.
[22] E141 Coll., Phys. Rev. Lett. 59 (1987) 755. E774 Coll., Phys. Rev. Lett. 67 (1991) 2942. MAMI/A1 Coll., Phys. Rev. Lett. 106 (2011) 251802. APEX Coll., Phys. Rev. Lett. 107 (2011) 191804. WASA Coll., Phys. Lett. B 726 (2013) 187. HADES Coll., Phys. Lett. B 731 (2014) 265271. A1 Coll., Phys. Rev. Lett. 112 (2014) 221802. BaBar Coll., arXiv:1406.2980.
[23] A. Anastasi *et al.* [KLOE-2], Phys. Lett. B **750** (2015) 633
[24] A. Anastasi *et al.* [KLOE-2], Phys. Lett. B **757** (2016) 356
[25] A. R. B. Batell, M. Pospelov, Phys. Rev. D 79 (2009) 115008.
[26] A. Anastasi *et al.* [KLOE-2], Phys. Lett. B **747** (2015) 365
[27] F. Jegerlehner, A. Nyffeler, Phys.Rept.477(2009)1
[28] D. Babusci *et al.* [KLOE-2], Phys. Lett. B **742** (2015) 1
[29] A. Anastasi *et al.* [KLOE-2], Phys. Lett. B **757** (2016) 362
[30] L.G. Landsberg, Phys. Rep.**128**(1985)301.
[31] S. Ivashyn, Prob. Atomic Sci. Technol. **2012N1**(2012)179.
[32] C. Terschlusen, S. Leupold, Phys. Lett. B**691**(2010)191.
[33] A. Anastasi *et al.* [KLOE-2 Coll.], JHEP **1605** (2016) 019